

## Electronic Supplementary Information (ESI)

### Photochemistry of 9-acridinecarboxaldehyde in aqueous media

Wolf-Ulrich Palm

Institute of Sustainable Chemistry and Environmental Chemistry

Leuphana University, Universitätsallee 1, 21335 Lüneburg, Germany.

Fax: +49 4131 677 2822; Tel: +49 4131 677 2874; E-mail: palm@uni.leuphana.de

#### Contents

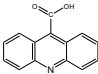
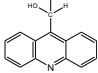
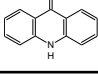
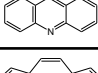
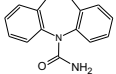
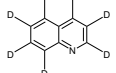
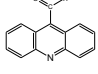
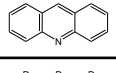
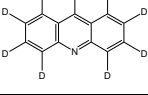
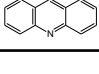
<b>1</b>	<b>Origin of compounds and properties</b>	<b>S2</b>
1.1	Structures, suppliers and purities . . . . .	S2
1.2	Properties of compounds . . . . .	S3
<b>2</b>	<b>Analysis by LC-MSMS</b>	<b>S4</b>
2.1	Conditions and parameters . . . . .	S4
2.2	Mass-spectra and purity of ACL . . . . .	S7
2.3	Formation of ACR in the ESI-head . . . . .	S9
2.4	Formation of ACH and correlation of ACL and ACH . . . . .	S10
<b>3</b>	<b>Kinetic scheme for the dark reaction</b>	<b>S12</b>
<b>4</b>	<b>Photolysis of ACL</b>	<b>S14</b>
4.1	Rate constants . . . . .	S14
4.2	Action-spectrum of ACL . . . . .	S14
4.3	Quantum yields at different pH-values . . . . .	S16
4.4	Photolysis of ACL with and without oxygen . . . . .	S16
4.5	UV-spectra of ACL in different solvents . . . . .	S18
4.6	Corrections performed in the sun-light photolysis . . . . .	S18
4.6.1	Input parameters for STARSci and for SMARTS . . . . .	S18
4.6.2	Correction by the dimension of the experimental setup . . . . .	S19

# 1 Origin of compounds and properties

## 1.1 Structures, suppliers and purities

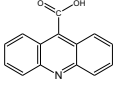
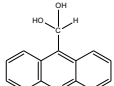
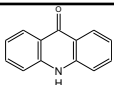
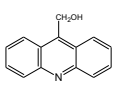
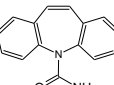
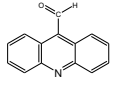
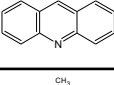
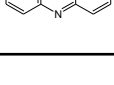
Structures, abbreviations, suppliers and purities of all compounds used in this study are summarized in Table S1, properties of all compounds in Table S2.

**Table S1** Compounds, structures, their abbreviation and suppliers with stated purities. abb = abbreviation used throughout the study, A = in equilibrium with ACL, B = purity obtained in this study. Order of compounds with increasing retention time (see Table S3).

structure	formula	CAS No	abb.	supplier	purity	note
9-Acridinecarboxylic acid monohydrate						
	C <sub>14</sub> H <sub>9</sub> NO <sub>2</sub>	5336-90-3	<b>ACA</b>	Aldrich	97 %	
1-(9-Acridinyl)-methanediol						
	C <sub>14</sub> H <sub>11</sub> NO <sub>2</sub>	159307-57-0	<b>ACH</b>	—	—	A
9(10H)-Acridinone						
	C <sub>13</sub> H <sub>9</sub> NO	578-95-0	<b>ACO</b>	Aldrich	99 %	
9-Acridinemethanol						
	C <sub>14</sub> H <sub>11</sub> NO	35426-11-0	<b>ACM</b>	synthesis	≈ 90 %	B
Carbamazepine						
	C <sub>15</sub> H <sub>12</sub> N <sub>2</sub> O	298-46-4	<b>CBZ</b>	Aldrich	98 %	
Quinoline-D7						
	C <sub>9</sub> D <sub>7</sub> N	34071-94-8ä	<b>IS1</b>	CDN	99 %	
9-Acridinecarboxaldehyde						
	C <sub>14</sub> H <sub>9</sub> NO	885-23-4	<b>ACL</b>	synthesis Aldrich	98 % 97 %	B
Acridine						
	C <sub>13</sub> H <sub>9</sub> N	260-94-6	<b>ACR</b>	Aldrich	97 %	
Acridine-D9						
	C <sub>13</sub> D <sub>9</sub> N	34749-75-2	<b>IS2</b>	CIL	98 %	
9-Methylacridine						
	C <sub>14</sub> H <sub>11</sub> N	611-64-3	<b>MAC</b>	Aldrich	95 %	

## 1.2 Properties of compounds

**Table S2** Properties of compounds (at room temperature, if not stated otherwise values from Scifinder, last access April 2018, \* = estimations). M = molar mass; MP = melting point;  $S_{H_2O}$  = solubility in water at pH = 7;  $\log(K_{OW})$  = logarithmic octanol-water coefficient;  $pK_a$  = logarithmic dissociation constant. A = this work. B = decomposition. C = base. D = acid. Order of compounds with increasing retention time (see Table S3).

structure	M g mol <sup>-1</sup>	MP °C	Lit	$S_{H_2O}$ mg L <sup>-1</sup>	$\log(K_{OW})$	$pK_a$	Lit
	223.23	279-280		16000*	2.93*	5.0 3	<sup>1</sup> C <sup>1</sup> D
	225.24	—		86*	2.4*	—	
	195.22	340-367		1.9*	3.23*	-0.32	<sup>2</sup>
	209.24	264 264-265	A B <sup>3</sup> B	80*	2.5*	5.24 ± 0.02	A C
	236.27	190.2		112*	2.45*	13.94*	
	207.23	138-150 145-147	A	8*	2.83*	4.30 ± 0.05 4.38 ± 0.04 4.52	<sup>4</sup> C A <sup>5</sup> C <sup>2</sup> C
	179.22	108		38.4*	3.4*	5.6 5.36	<sup>1</sup> C <sup>2</sup> C
	193.24	110-130		60*	3.99*	5.76	<sup>2</sup> C

## 2 Analysis by LC-MSMS

### 2.1 Conditions and parameters

Compounds were analysed by LC-MSMS (HPLC 1200 (Agilent) with dual pump, autosampler, column oven and MSMS 6430 (Agilent)).

Conditions HPLC: column Macherey Nagel 125/3.0 Nucleodur C18 PAH 3  $\mu\text{m}$ , isocratic eluent 40 % 1 mM ammonium acetate / 60 % acetonitrile,  $T = 40\text{ }^{\circ}\text{C}$ , injection volume = 5  $\mu\text{L}$ , flow rate = 0.4 ml/min. Post column addition with 10  $\mu\text{L}/\text{min}$  of a 1 % formic acid with a second HPLC-pump. The addition of formic acid is necessary for the internal standard quinoline-D7 leading to increased signals by about a factor of 20 with respect to an analysis without post addition of acid.

Conditions MS: ESI-head, positive mode. Source parameters:  $T = 350\text{ }^{\circ}\text{C}$ , gas flow = 10 L/min,  $p(\text{nebulizer}) = 35\text{ psi}$ , capillary voltage = 4000 V.

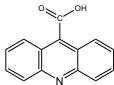
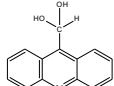
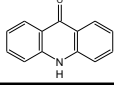
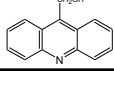
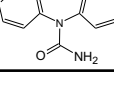
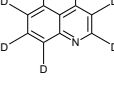
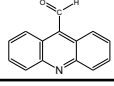
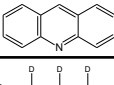
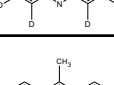

LC-MSMS parameter are summarized in Table S3 and transitions of all compounds investigated in the LC-MSMS analysis are shown in Figure S1.

As shown in Figure S1 in some cases protonated acridine derivatives are formed in the ESI-head from their parent compounds.

- Acridine (ACR) is formed from 9-acridinecarboxaldehyde (ACL) and the hydrate of ACL (ACH)
- 9-Acridinemethanol (ACM) is formed from ACL
- ACH is formed from ACL
- 9-Methylacridine (MAC) is formed from carbamazepine (CBZ)

Especially both the formation of ACR from ACL and the equilibrium of ACH with ACL on the analysis of ACL are discussed in section 2.3 and section 2.4.

**Table S3** LC-MSMS parameter (Agilent 6430, positive mode) and typical retention times (conditions see text). Precursor = protonated molecular mass  $[MH]^+$ , product = protonated fragment from precursor. transition = transitions for quantifier (qual) and qualifier (qual), CE = collision energy, FV = fragmentor voltage, RT = retention time. Order of compounds with increasing retention time.

structure	transition	precursor m/z	product m/z	CE V	FV V	RT min
	quan qual	224	196 180	28 30	132	0.95
	quan qual	226	180 208	28 30	150	1.35
	quan qual	196	167 139	37 40	160	1.68
	quan qual	210	180 167	28 30	150	1.81
	quan qual	237	194 192	20 20	140	1.83
	quan qual	137	109 133	30 30	160	2.80
	quan qual	208	180 152	31 30	122	3.66
	quan qual	180	152 128	36 40	158	4.62
	quan qual	189	133 159	42 42	180	4.62
	quan qual	194	193 179	32 40	152	6.19

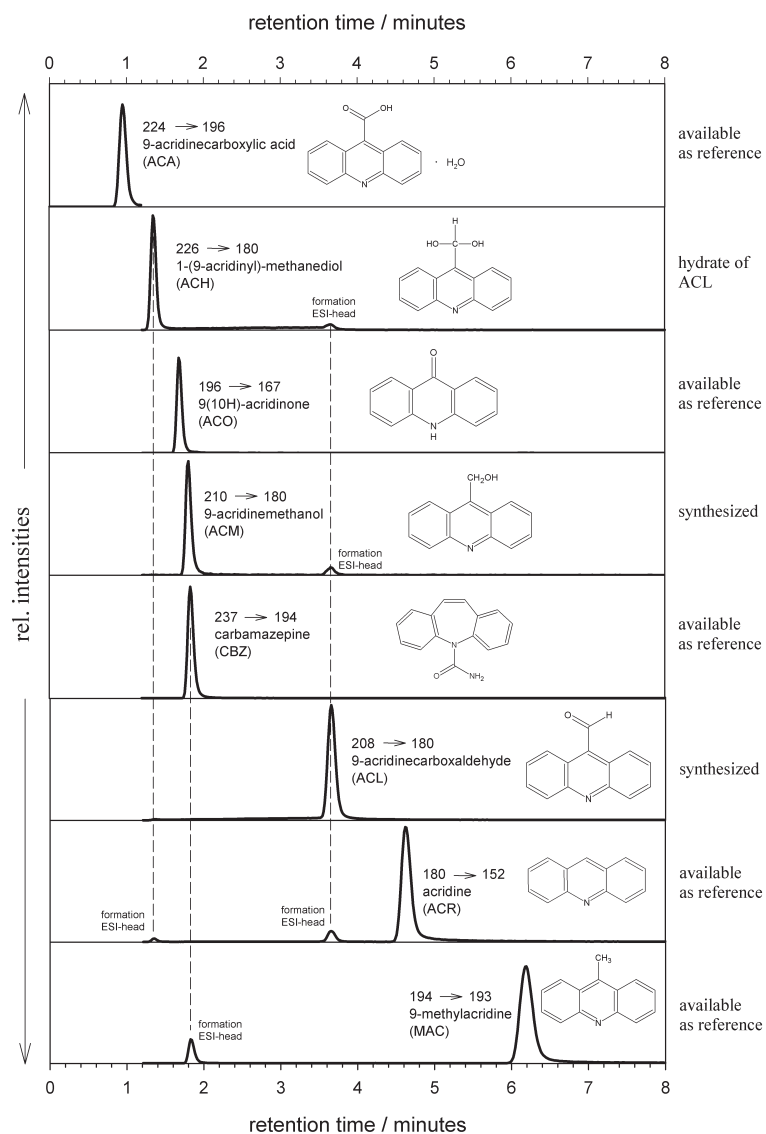


**Fig. S1** LC-MS/MS peaks for transitions of all compounds (with the exception of internal standards quinoline-D7 and acridine-D9), summarized in Table S3.

## 2.2 Mass-spectra and purity of ACL

Mass spectra obtained with a fragmentor voltage of 130 V of ACR, ACL, ACM, ACO, ACH and ACA are shown in Figure S2. Impurities and their amounts (calculated from available reference compounds) in a typical dark sample of ACL are shown in Figure S3. Purity of ACL after recrystallisation was estimated to be about 98%.

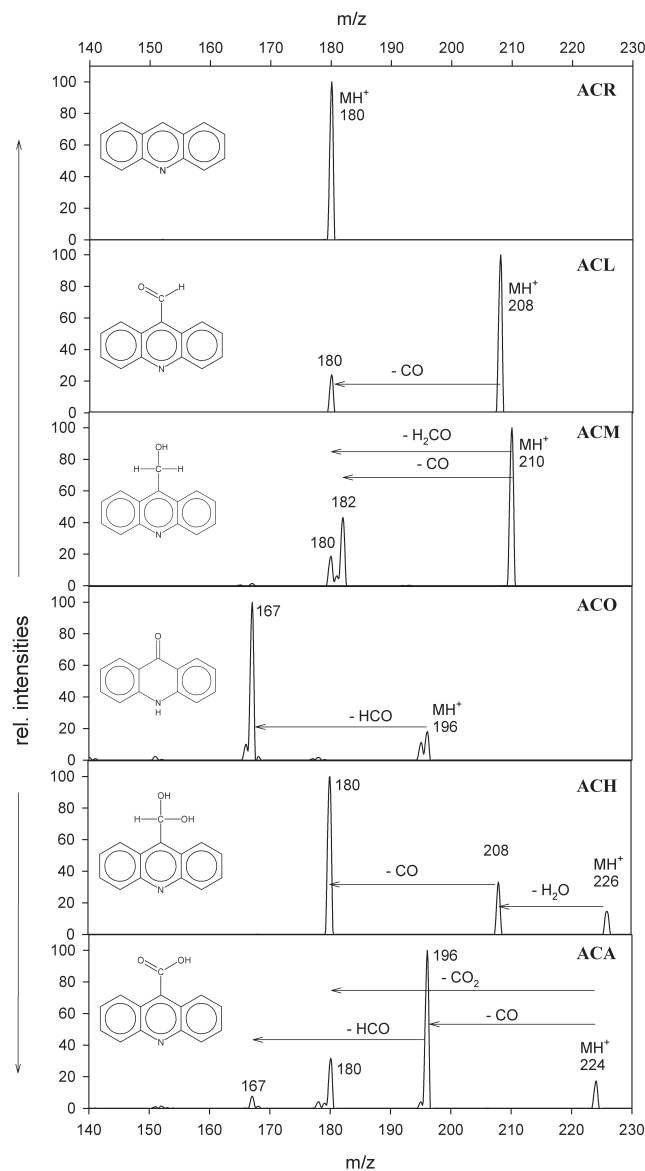


**Fig. S2** Mass spectra obtained with a fragmentor voltage of 130 V of ACR, ACL, ACM, ACO, ACH and ACA.

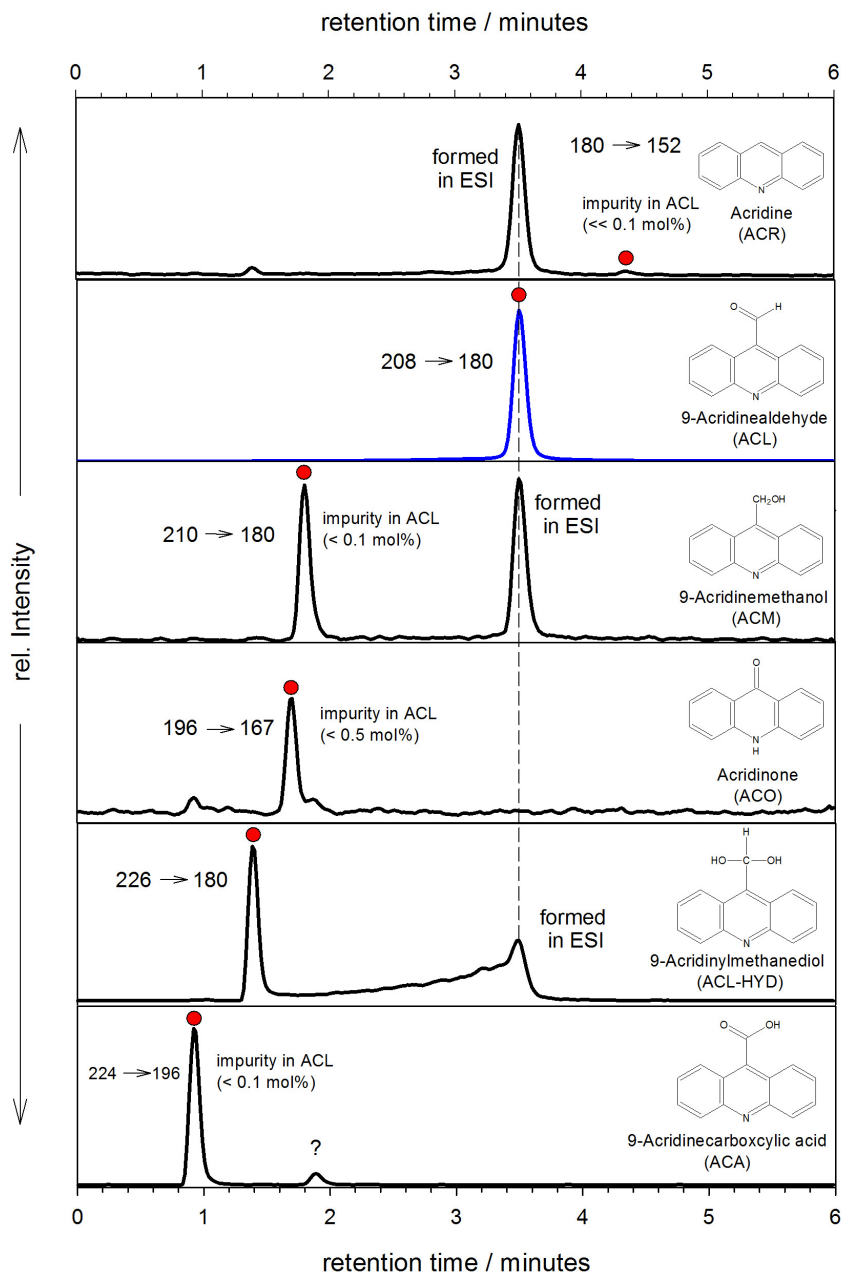


**Fig. S3** Chromatograms of impurities and their amount (in mol %) in a typical dark sample of 9-acridinecarboxaldehyde (ACL,  $c = 1 \text{ mg/L} = 4.83 \text{ } \mu\text{M}$ ). Carbamazepine and 9-methylacridine were always found below the detection limit (i.e.  $< 1 \text{ } \mu\text{g L}^{-1}$ ) in dark samples of ACL and transitions of these two compounds are not shown. Peaks for ACL and ACH and of impurities are labeled with a red dot. Signals of acridine and 9-acridinemethanol at the retention time of ACL indicate a formation in the ESI head. Considering the indicated amount of impurities the purity of ACL is assumed to be  $\geq 98\%$ .



### 2.3 Formation of ACR in the ESI-head

Acridine (ACR) is formed in the ESI-head from 9-acridinecarboxaldehyde (ACL) for the conditions described in section 2.1. ACR is detected on the trace of ACR  $180 \rightarrow 152$  at the retention time of ACL (RT = 3.66 minutes). The correlation of the absolute concentrations of  $c(\text{ACR})$  versus  $c(\text{ACL})$  is shown in Figure S4. The amount of ACR formed in the ESI-head from ACL is linearly correlated with the start concentration of ACL. Calibrations of all compounds were performed using the nominal start concentrations, respectively and discarding any loss in the ESI-head. Hence, analysis of all compounds is only valid for the conditions used.

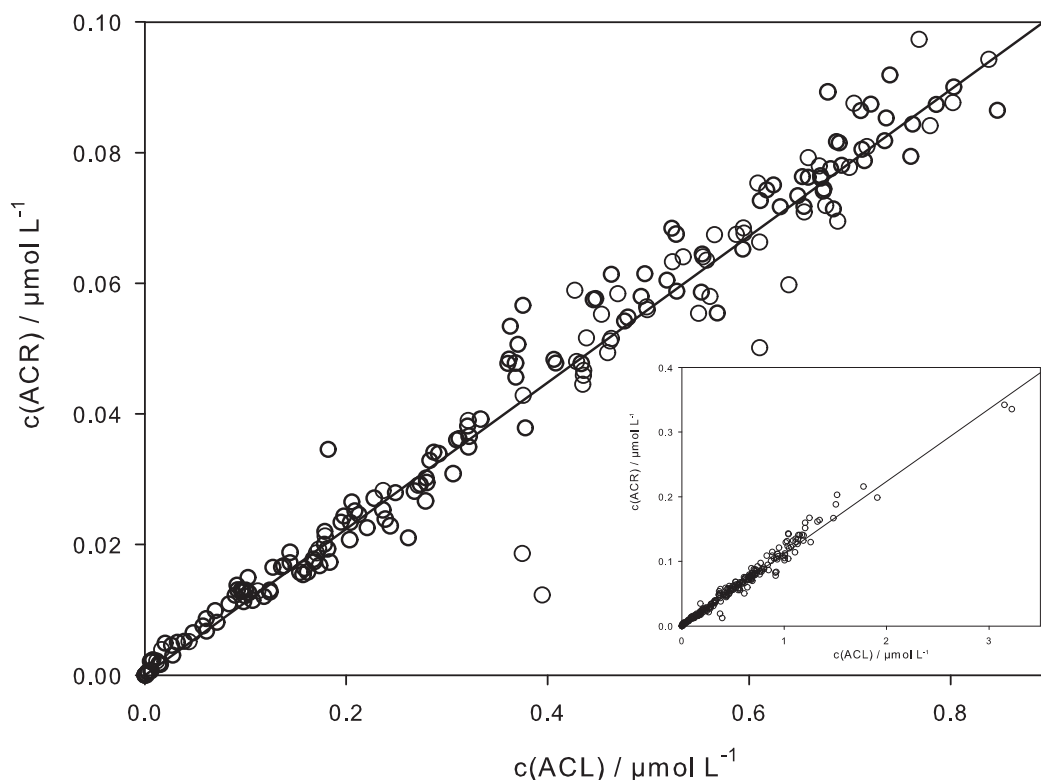


**Fig. S4** Correlation of the concentration of acridine  $c(\text{ACR})$  formed in the ESI-head from 9-acridinecarboxaldehyde (ACL) with the concentration  $c(\text{ACL})$ . Shown are concentrations of acridine (transition  $180 \rightarrow 152$ ) at the retention time of ACL (RT = 3.66 minutes, 14 experiments, N=237).

## 2.4 Formation of ACH and correlation of ACL and ACH

Due to changing temperatures, pH-values and solvents, the equilibrium of ACL and ACH is disturbed during the analytical run on the column, leading to broad signals in the LC analysis. This phenomenon was already described in<sup>6</sup>. Equilibrium constants and rate constants of the hydrolysis and formation of ACH are given in<sup>4</sup>. Relative concentrations of ACL, the protonated form of ACL ( $\text{ACLH}^+$ ) and ACH and the protonated form of ACH ( $\text{ACHH}^+$ ), calculated with the data given in<sup>4</sup>, are shown in Figure S5.

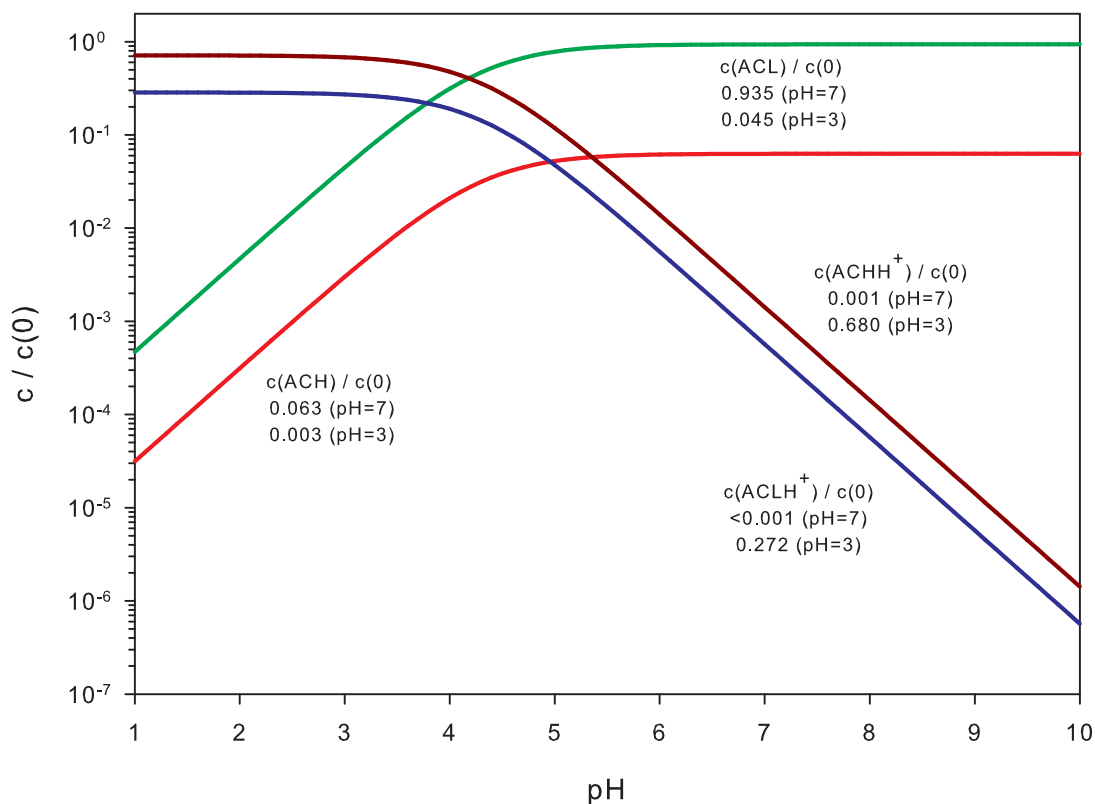


**Fig. S5** pH-dependence of the fractions of  $c(\text{ACL})$ ,  $c(\text{ACLH}^+)$  and for the hydrate of ACL  $c(\text{ACH})$  and  $c(\text{ACHH}^+)$  calculated from data given in<sup>4</sup>.

With the exception for measurements of pH dependent quantum yields all measurements were performed for  $\text{pH} > 5.5$  and samples were analyzed with a neutral eluent (ammonium acetate/acetonitrile) with a column temperature of  $T = 40^\circ\text{C}$  (LC-MSMS conditions see section 2.1). The concentration of the hydrate ACH increases with decreasing pH (see Figure S5). An example of chromatograms for samples at low and high pH is shown in Figure S6.

The linear correlation of LC-MSMS areas found for ACH versus areas of ACL is shown in Figure S7 using dark and photolysis samples from measurements in water or at  $\text{pH}=7$  with maximum concentrations of ACL of  $c(\text{ACL}) = 6 \mu\text{M}$  ( $N = 259$ ). From the linear regression slope =  $\text{area}(\text{ACH}) / \text{area}(\text{ACL}) = 0.05$ . With  $\text{response}(\text{ACH}) \approx 0.5 \times \text{response}(\text{ACL})$  concentrations for ACH are  $c(\text{ACH}) \approx 0.1 \times c(\text{ACL})$ , i.e. about 10% of ACH relative to ACL is present. These assumed concentrations of ACH are in agreement with data given in<sup>4</sup> with fractions of ACH in the range of 6 - 10 % for pH-values  $5.5 \leq \text{pH} \leq 10$ , see Figure S5.

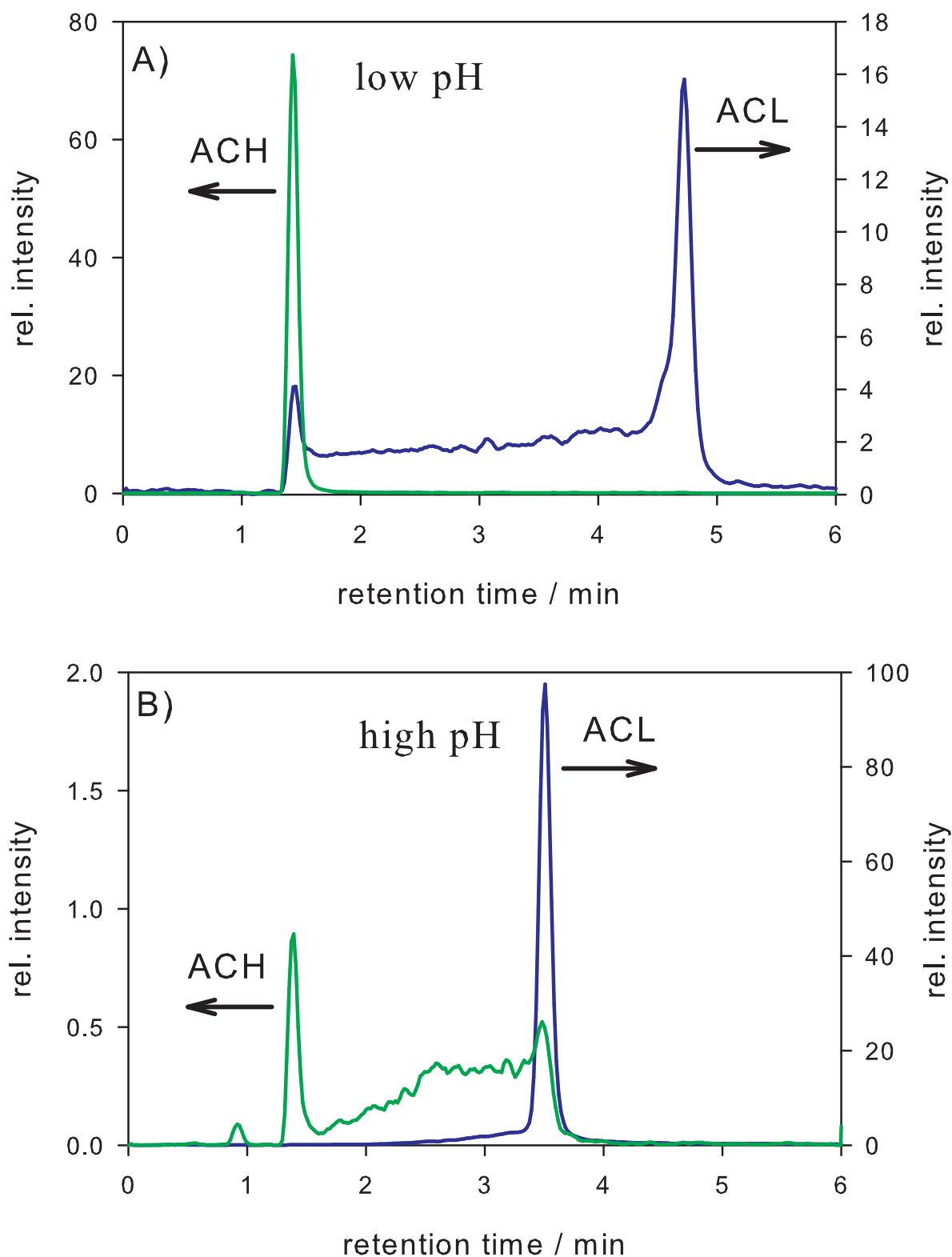


**Fig. S6** Chromatograms for transitions from ACH and ACL at different pH-values with the analysis parameter given in section 2.1. (A) sample pH=3, column temperature  $T = 23\text{ }^{\circ}\text{C}$ , (B) sample pH=7.7, column temperature  $T = 40\text{ }^{\circ}\text{C}$ .

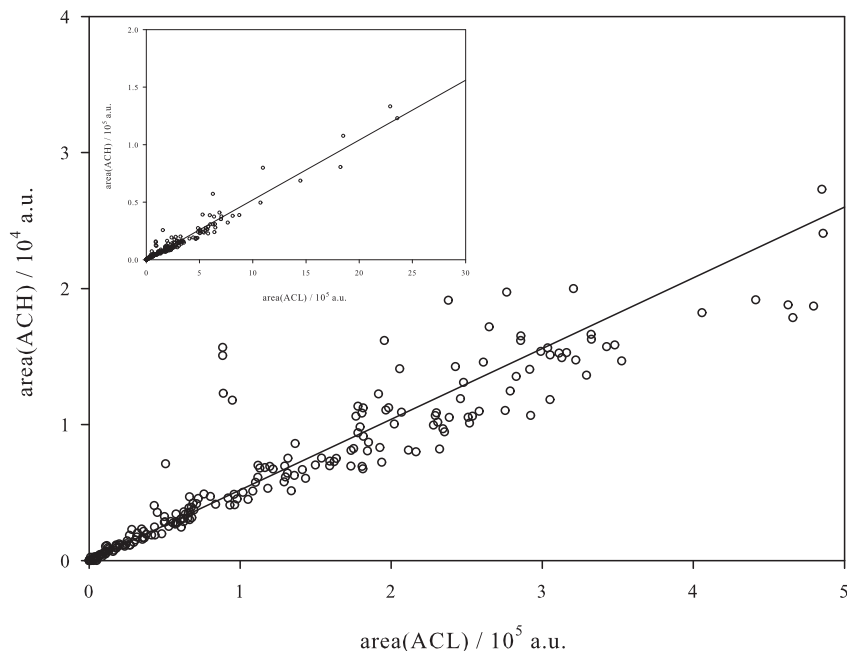


**Fig. S7** Correlation of LC-MSMS areas found for the hydrate of ACL (ACH) versus areas of 9-acridinecarboxaldehyde (ACL). Samples from measurements in water or at pH=7 including dark and photolysis samples (N = 259). Linear regression leads to slope =  $\text{area(ACH)} / \text{area(ACL)} = 0.05$ . With  $\text{response(ACH)} \approx 0.5 \times \text{response(ACL)}$  concentrations for ACH are  $c(\text{ACH}) \approx 0.1 \times c(\text{ACL})$ , i.e. about 10% of ACH relative to ACL is present.

### 3 Kinetic scheme for the dark reaction

The kinetics of a parallel reaction of 1st and 2nd order is discussed in detail in textbooks<sup>7, 8</sup>. Solutions for all integrals and calculations were checked with the program package *Mathematica*. With the exception of 9-acridinecarboxaldehyde (ACL) with  $c_0(\text{ACL}) = 1.2 \mu\text{mol/L}$  all other start concentrations of products were found to be negligible, i.e.  $c(\text{ACA}0) = c(\text{ACM}0) = c(\text{ACR}0) = 0$ .

Two products were found in the dark reaction of ACL in the aqueous phase (a) 9-acridinecarboxylic acid (ACA) as main product and (b) the minor product 9-acridinemethanol (ACM).

Experiments were performed at  $T = 20^\circ\text{C}$  at pH=7 in oxygen saturated solution ( $c_{\text{O}_2} = 8.3 \text{ mg/L} = 2.6 \cdot 10^{-4} \text{ M}$ ). Oxygen concentrations are therefore about a factor of 200 higher compared to the start concentration of ACL and with respect to a reaction with oxygen a 1st-order reaction can be assumed. The main part of ACA can be assumed to be formed due to oxidation by molecular oxygen (reaction S3.1), the formation of ACM can be assumed to be formed (together with an equimolar concentration of ACA) by a Cannizzaro-type reaction (reaction S3.2).



The solution of the differential equation for  $c(ACL)$

$$\frac{dc(ACL)}{dt} = -k_{1d} \cdot c(ACL) - 2 \cdot k_{2d} \cdot c(ACL)^2 \quad (S3.3)$$

is

$$c(ACL) = \frac{c(ACL0) \cdot k_{1d} \cdot e^{-k_{1d} \cdot t}}{2 \cdot k_{2d} \cdot c(ACL0) - 2 \cdot k_{2d} \cdot c(ACL0) \cdot e^{-k_{1d} \cdot t} + k_{1d}} \quad (S3.4)$$

With the definition<sup>7</sup>

$$\kappa = \frac{2 \cdot k_{2d} \cdot c(ACL0)}{k_{1d}} \quad (S3.5)$$

equation (S3.4) leads to

$$c(ACL) = \frac{c(ACL0) \cdot e^{-k_{1d} \cdot t}}{1 + \kappa - \kappa \cdot e^{-k_{1d} \cdot t}} \quad (S3.6)$$

and with  $A = e^{-k_{1d} \cdot t}$  and  $B = 1 + \kappa - \kappa \cdot e^{-k_{1d} \cdot t}$

$$c(ACL) = \frac{c(ACL0) \cdot A}{B} \quad (S3.7)$$

The solution of the differential equation for  $c(ACA)$

$$\frac{dc(ACA)}{dt} = k_{1d} \cdot c(ACL) + k_{2d} \cdot c(ACL)^2 \quad (S3.8)$$

with the abbreviations given above is

$$c(ACA) = \frac{c(ACL0)}{2} \cdot \left( 1 - \frac{A}{B} + \frac{1}{\kappa} \cdot \ln(B) \right) \quad (S3.9)$$

The solution of the differential equation for  $c(ACM)$

$$\frac{dc(ACM)}{dt} = k_{2d} \cdot c(ACL)^2 \quad (S3.10)$$

with the abbreviations given above is

$$c(ACM) = \frac{c(ACL0)}{2} \cdot \left( 1 - \frac{A}{B} - \frac{1}{\kappa} \cdot \ln(B) \right) \quad (S3.11)$$

Equations (S3.7), (S3.9) and (S3.11) lead to the mass balance:

$$c(ACL0) = c(ACM) + c(ACA) + c(ACL) \quad (S3.12)$$

Equations (S3.7) for ACL, (S3.9) for ACA and (S3.11) for ACM are used in the main text in the discussion of the concentration dependent measurements.

## 4 Photolysis of ACL

### 4.1 Rate constants

Rate constants  $k_P$  for the photolysis of ACL in aqueous solution in series A - D are summarized in Table S4. Rate constants for the loss of ACL ( $k_P$ ) and the formation of ACR ( $k_{ACR}$ ) and ACA ( $k_{ACA}$ ) and corresponding yields were obtained from a fit assuming 1st-order reactions (i.e. from monoexponential functions) for a given start concentration  $c_0$ .

### 4.2 Action-spectrum of ACL

An example of an action spectrum of ACL in water with data for the spectral photon flux of the xe-light source used in the laboratory is shown in Figure S8. For the calculation of the rate constant  $k_P$  a quantum yield of  $\Phi_{ACL} = 0.015 \text{ mol mol}^{-1}$  was used.

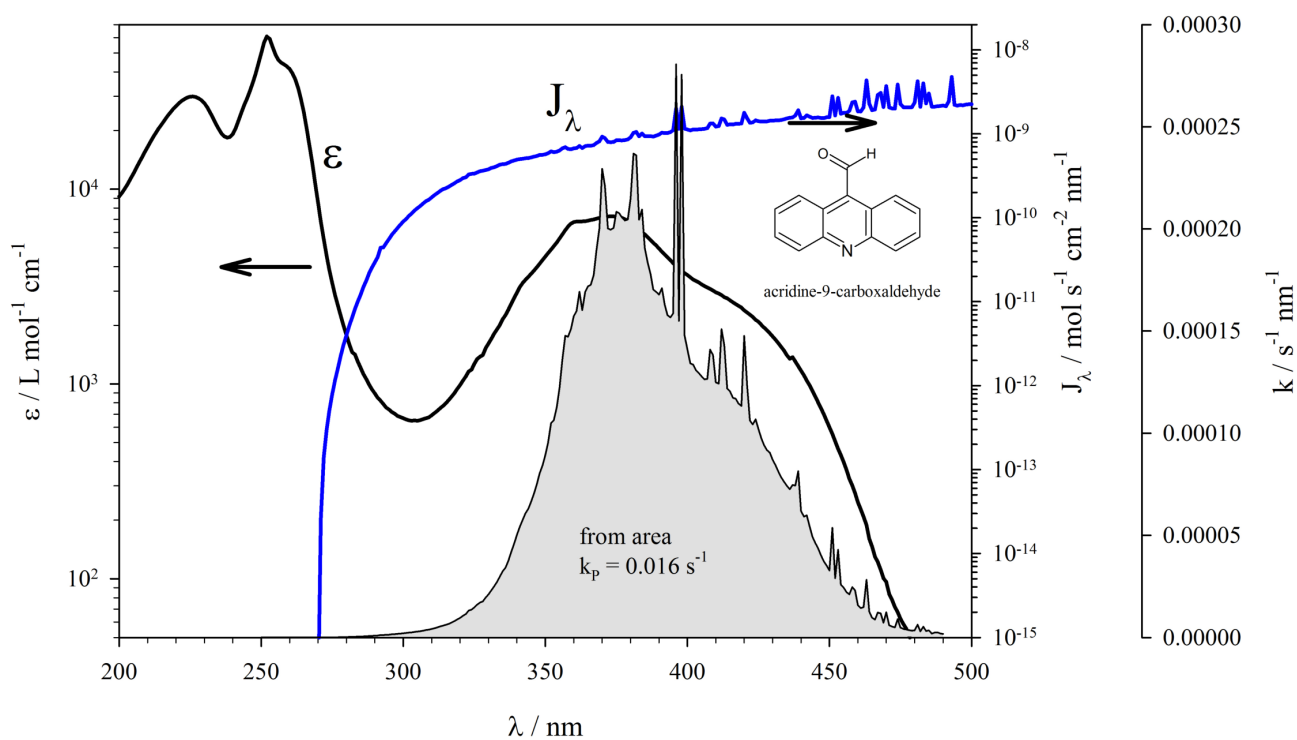


**Fig. S8** Action spectrum of ACL with the spectral photon flux of the xe-light source in the laboratory.

**Table S4** Monoexponential rate constants  $k_P$  for the photolysis of ACL, for the formation of ACR and ACA and corresponding yields of ACR and ACA in aqueous solution. Shown are results from 4 independent series.

No	$c_0$ $\mu\text{M}$	$k_P$ $\text{s}^{-1}$	$k_{ACR}$ $\text{s}^{-1}$	$k_{ACA}$ $\text{s}^{-1}$	yield ACR   ACA	$r^2$	series and comment
1	1.93	$0.020 \pm 0.0002$	$0.019 \pm 0.0001$	$0.0006 \pm 0.00007$	0.97   0.03	0.9994	A, air saturated, water
2	1.93	$0.018 \pm 0.0004$	$0.020 \pm 0.0003$	$0.0005 \pm 0.00013$	1.13   0.03	0.9979	A, air saturated, water
3	1.93	$0.018 \pm 0.0003$	$0.020 \pm 0.0002$	$0.0003 \pm 0.00010$	1.09   0.02	0.9988	A, air saturated, water
4	1.93	$0.020 \pm 0.0006$	$0.019 \pm 0.0004$	$0.0003 \pm 0.00021$	0.94   0.02	0.9994	A, air saturated, water
5	0.18	$0.015 \pm 0.0005$	$0.015 \pm 0.0004$	$0.0002 \pm 0.00017$	0.96   0.02	0.9960	B, air saturated, water
6	0.73	$0.011 \pm 0.0002$	$0.011 \pm 0.0002$	$0.0004 \pm 0.00010$	0.97   0.03	0.9977	B, air saturated, water
7	1.49	$0.016 \pm 0.0005$	$0.014 \pm 0.0004$	$0.0009 \pm 0.00017$	0.88   0.06	0.9961	B, air saturated, water
8	4.04	$0.013 \pm 0.0003$	$0.009 \pm 0.0002$	$0.0009 \pm 0.00012$	0.70   0.07	0.9962	B, air saturated, water
9	9.03	$0.015 \pm 0.0003$	$0.008 \pm 0.0002$	$0.0017 \pm 0.00011$	0.54   0.11	0.9963	B, air saturated, water
10	16.59	$0.012 \pm 0.0003$	$0.006 \pm 0.0001$	$0.0029 \pm 0.00012$	0.47   0.24	0.9940	B, air saturated, water
11	4.83	$0.015 \pm 0.0003$	$0.013 \pm 0.0002$	$0.0032 \pm 0.00012$	0.83   0.21	0.9970	C, N <sub>2</sub> saturated, water
12	4.83	$0.019 \pm 0.0002$	$0.013 \pm 0.0001$	$0.0042 \pm 0.00009$	0.72   0.22	0.9988	C, air saturated, water
13	4.83	$0.016 \pm 0.0002$	$0.013 \pm 0.0001$	$0.0031 \pm 0.00008$	0.79   0.19	0.9989	C, O <sub>2</sub> saturated, water
14	1.41	$0.018 \pm 0.0001$	$0.017 \pm 0.0001$	$0.0006 \pm 0.00003$	0.98   0.04	0.9999	D, air saturated, pH=7.0
15	1.52	$0.017 \pm 0.0004$	$0.017 \pm 0.0003$	$0.0007 \pm 0.00012$	0.97   0.04	0.9994	D, air saturated, pH=6.1
16	1.45	$0.021 \pm 0.0005$	$0.019 \pm 0.0004$	$0.0011 \pm 0.00016$	0.91   0.05	0.9992	D, air saturated, pH=5.4
17	1.64	$0.035 \pm 0.0010$	$0.031 \pm 0.0009$	$0.0022 \pm 0.00020$	0.89   0.06	0.9995	D, air saturated, pH=3.9
18	1.76	$0.035 \pm 0.0011$	$0.033 \pm 0.0010$	$0.0017 \pm 0.00020$	0.94   0.05	0.9994	D, air saturated, pH=2.9

### 4.3 Quantum yields at different pH-values

Degree of dissociation of the base  $ACLH^+$ , calculated from  $pK_a \pm \sigma = 4.38 \pm 0.04$  obtained in this study (for a comparison with literature values see Table S2) and quantum yields of the photoreaction of ACL at different pH-values between pH = 3 - 7 are shown in Figure S9.

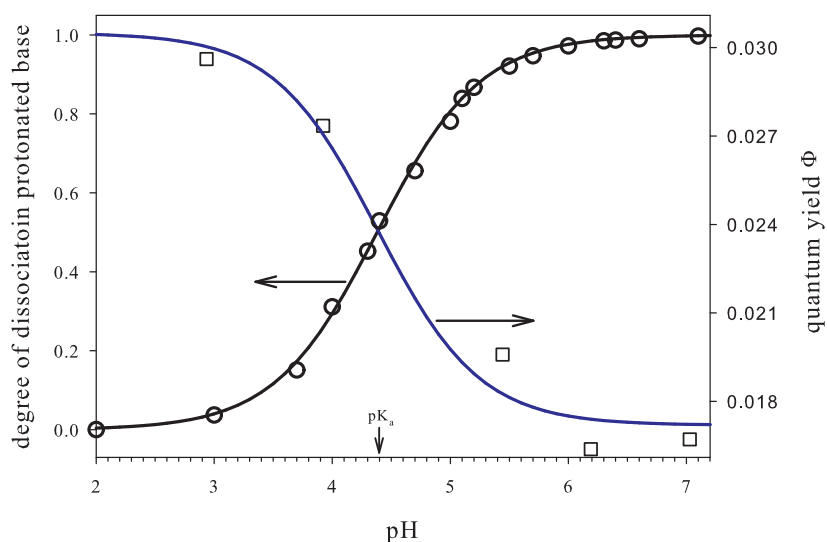


**Fig. S9** Degree of dissociation of the base  $ACLH^+$ , calculated from the  $pK_a$  and quantum yields at 5 different pH-values between pH = 2 - 7.

### 4.4 Photolysis of ACL with and without oxygen

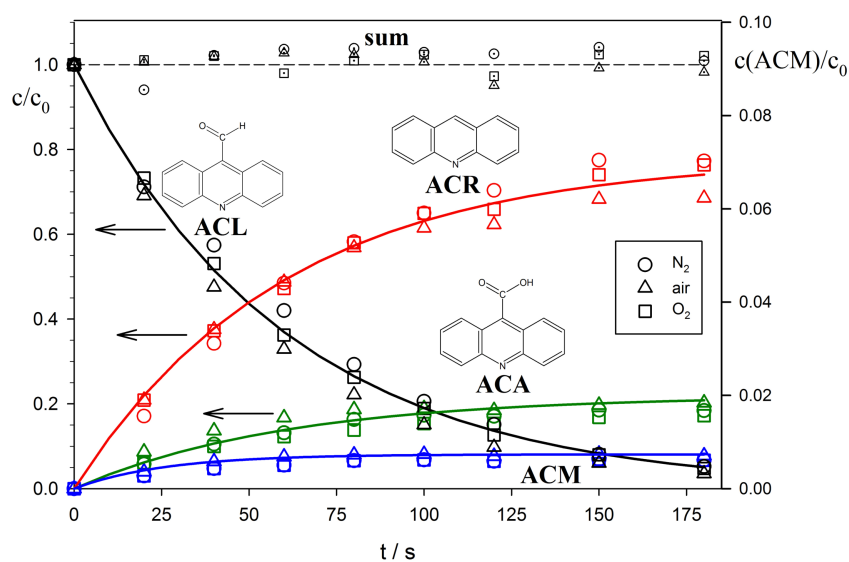


**Fig. S10** Photolysis of ACL ( $c_0 = 4.83 \mu\text{M}$ ) in aerated solutions with  $\text{N}_2$ , air and  $\text{O}_2$ . Note the reduced scale for ACM (right axis) by a factor of 10.



The kinetics of the photolysis of ACL in aerated solutions with  $N_2$ , air and  $O_2$  is shown in Figure S10 together with the evolution of products ACR, ACA and ACM. Within the error of experiments oxygen concentration has a negligible influence on the photoreaction of ACL in aqueous solutions. Figure S10 also serves as an example that only low concentrations of ACM (maximum 1 % of start concentration of ACL) were found in photolysis experiments of ACL in aqueous solution.

Only negligible concentrations of 9(10H)-acridinone (ACO,  $c < 2\%$  of  $c_0(ACL)$ ) were found in all photolysis reactions and also in dark reactions of ACL, proved by an authentic sample of ACO. Although the photolysis of ACL is not influenced by oxygen, the formation of an unknown product strongly influenced by oxygen was found. This unknown (assumed minor) product was found on the trace for the transition of ACO (see Table S3). The evolution of this product (Figure S11) was obtained from photolysis experiments already shown in Figure S10. Relative concentrations of the unknown product in Figure S11 were calculated with the same response factor found for ACO. However, no further attempts were performed to identify this product. A suggestion for the product is 1-hydroxyacridine (or rather the more stable tautomeric acridinone<sup>9</sup>), possibly formed in a Norrish-Type II reaction from the intramolecular reduction of the aldehyde with subsequent reaction of the biradical with oxygen.

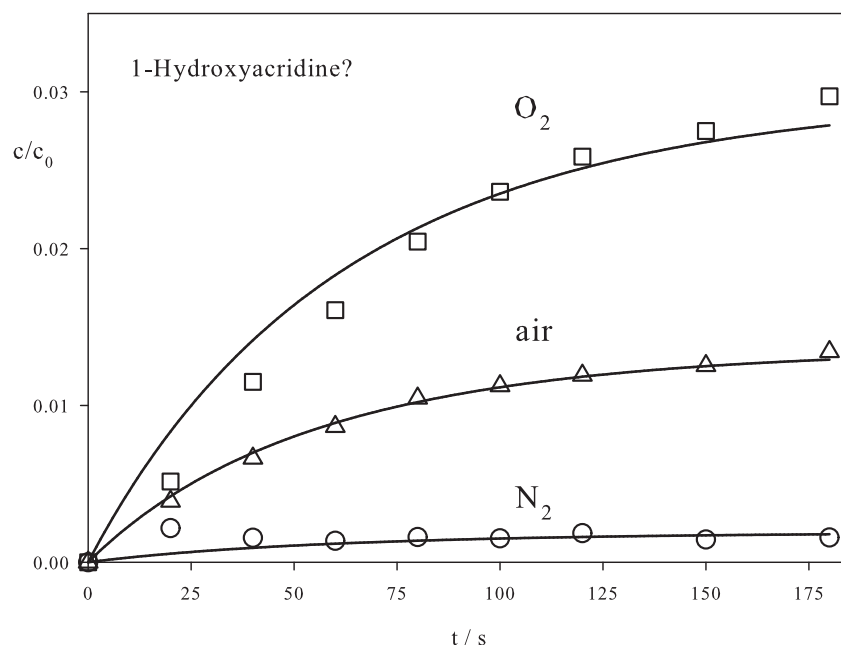


**Fig. S11** Evolution of an unknown product on the trace of the LC-MSMS transition for 9(10H)-acridinone (ACO) in the photolysis of ACL shown in Figure S10. Lines are from monoexponential fits, respectively. Concentrations relative to the start concentration of ACL were calculated with a response factor assumed to be identical to ACO.

## 4.5 UV-spectra of ACL in different solvents

UV-spectra of ACL in water, methanol, isopropanol, acetone and acetonitrile are shown in Figure S12.

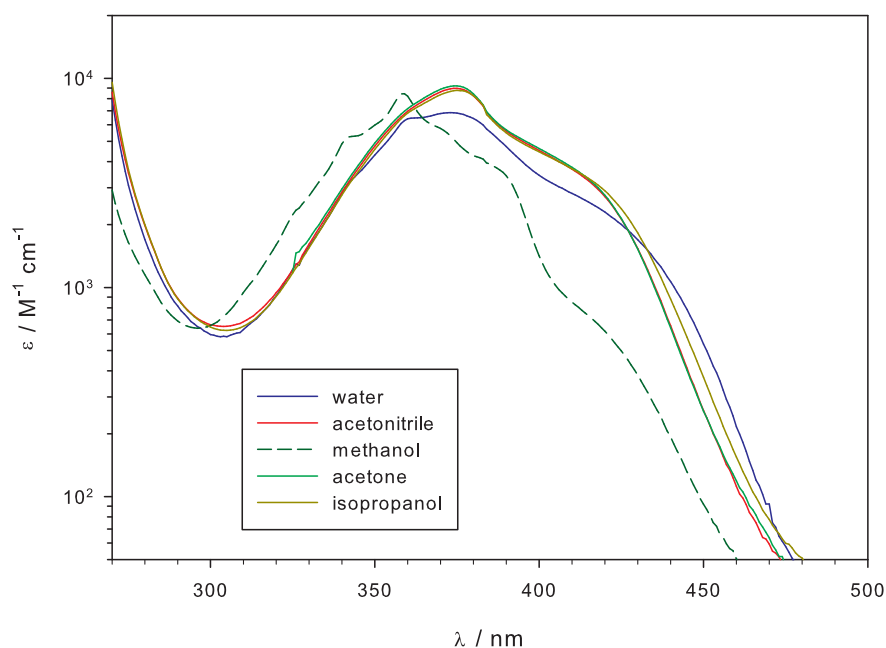


**Fig. S12** UV-spectra of ACL in different solvents. The quantum yield of ACL was determined in all solvents (see main text).

## 4.6 Corrections performed in the sun-light photolysis

### 4.6.1 Input parameters for STARSci and for SMARTS

Input parameters for STARSci in the calculation of the rate constant  $k_{clear\ sky}$ :

- the experimental values for temperature, rel. humidity and pressure,
- albedo characteristics for dry green grass,
- an aerosol optical depth at 550 nm of AOD=0.1,
- an ozone column concentration of 276 DU.

Input parameters for SMARTS in the calculation of the rate constant  $k_{clouds}$ :

- the experimental values for temperature, rel. humidity and pressure,
- the solar spectrum from Wehrli/WRC/WMO (1985) with a solar constant of 1367 W/m<sup>2</sup>,
- albedo characteristics for dry green grass,
- a tropospheric aerosol model with an aerosol optical depth at 550 nm of AOD=0.1,
- an ozone column concentration of 276 DU and  $c(\text{CO}_2) = 405$  ppmV.

#### 4.6.2 Correction by the dimension of the experimental setup

Due to the dimension of the experimental setup, i.e. the petri dish, a part of the sample will not be irradiated. In addition reflection from the water surface will reduce the solar irradiance. To estimate the reduction of the irradiance it is rational to divide the solar irradiance into a diffuse and direct part. Experimental data of the diffuse fraction of the solar irradiance  $D_{dif}$  are not available at the meteorological station and  $D_{dif}$  was estimated as mean value from two published correlations<sup>10,11</sup>. With the reflected fraction ( $0 \leq R \leq 1$ , diffuse part  $R_{dif}$  and direct part  $R_{dir}$ ) and a correction value  $C$  defined by the dimensions of the petri dish used ( $0 \leq C \leq 1$ , diffuse part  $C_{dif}$  and direct part  $C_{dir}$ ) two correction factors for the direct ( $F_{dir}$ ) and diffuse ( $F_{dif}$ ) part of the solar irradiance are defined in equations S4.13 and S4.14.

$$F_{dir} = (1 - D_{dif}) \cdot (1 - R_{dir}) \cdot C_{dir} \quad (S4.13)$$

$$F_{dif} = D_{dif} \cdot (1 - R_{dif}) \cdot C_{dif} \quad (S4.14)$$

The corrected rate constant  $k_{corr}$  is defined by equation S4.15.

$$k_{corr} = k_{clouds} \cdot (F_{dir} + F_{dif}) \quad (S4.15)$$

The reflected fraction  $R$  was calculated from the Snellius- and Fresnel-equations in dependence from the solar altitude (see also<sup>12</sup>). For the diffuse part  $R_{dif}$  a weighted solar altitude was used from a spherical segment of the hemisphere. The spherical segment is defined by an angle  $\alpha$  between the sampling point and the mean height of the nearest objects at the horizon. Due to the vegetation-free area on the airfield a small angle  $\alpha = 5^\circ$  was estimated and used in the calculation leading to a constant value for  $R_{dif} = 0.88$ .

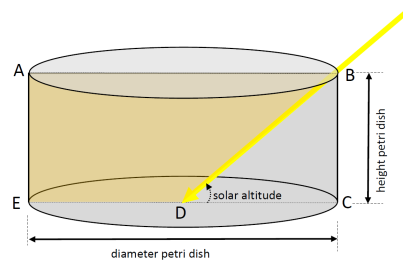


**Fig. S13** Scheme of the petri dish used in the definition of  $C_{dir}$  and  $C_{dif}$ .

For the correction by the dimensions of the petri dish Figure S13 should serve as a helpful scheme. The irradiated part of the solution in the petri dish is simply estimated from the fraction of the area  $F_1$  defined by the points ABDE and the area  $F_2$  defined by the rectangle ABCE (see Figure S13 and equation S4.16).

$$C_{dir} = \frac{F_1}{F_2} \quad (S4.16)$$

For the diffuse case the same arguments as above lead with the fraction of the spherical segment of  $1 - \cos(90 - \alpha) = 0.91$  to a constant value for  $C_{dif} = 0.91$ . All time dependent corrections for the day (5.9.2017) are summarized in Figure S14 with a mean correction factor over the day of  $\overline{F_{dir} + F_{dif}} = 0.74$

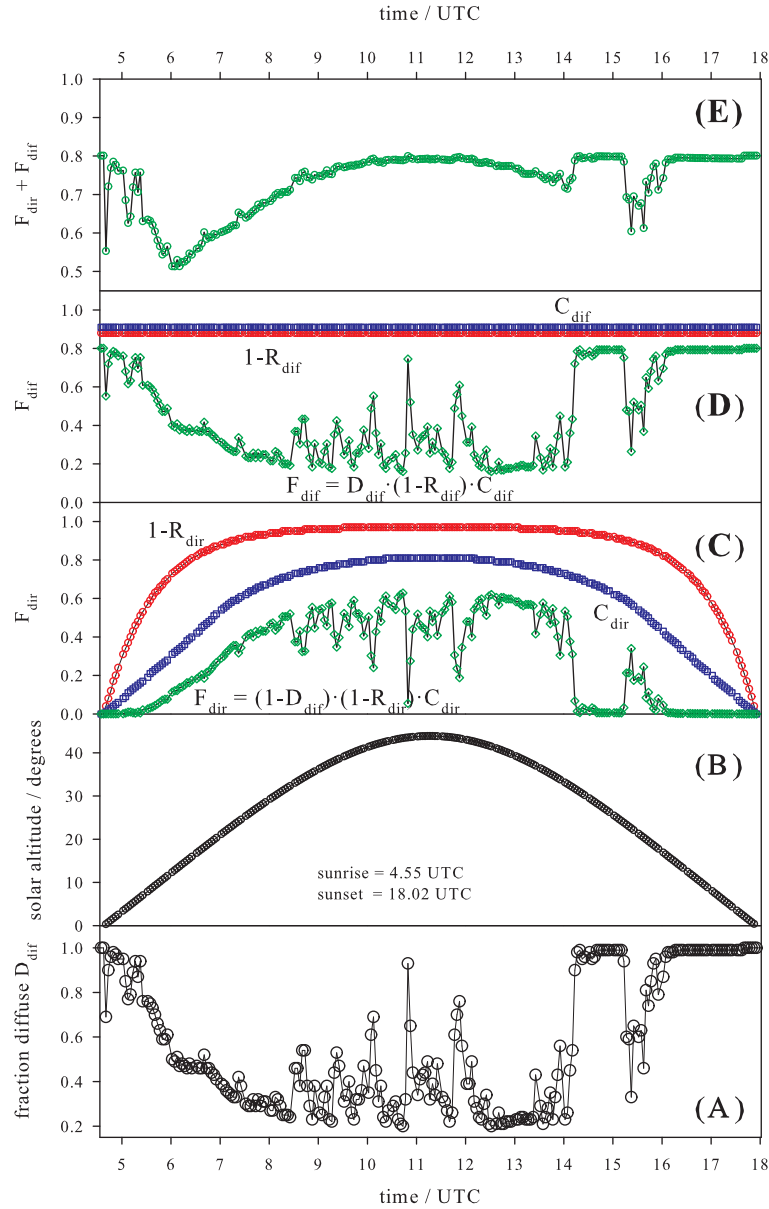


**Fig. S14** Correction factors versus time of day (in UTC) with a time resolution of 3 minutes calculated with meteorological data valid for the station at the airfield in Lüneburg (Germany) at September 5, 2017. (A) Calculated diffuse fraction  $D_{dif}$ , (B) solar altitude in degrees, (C) correction factors for the direct part of the solar irradiance, (D) correction factors for the diffuse part of the solar irradiance, (E) sum of correction factors  $F_{dir} + F_{dif}$ .

## References

- 1 A. Albert and R. Goldacre, *J. Chem. Soc.*, 1946, 706–713.
- 2 M. D. Mosher and E. Johnson, *Heterocycl. Commun.*, 2003, **9**, 555–558.
- 3 A. Campbell, C. S. Franklin, E. N. Morgan and D. J. Tivey, *J. Chem. Soc.*, 1958, 1145–1149.
- 4 R. A. McClelland, P. Sukhai, K. M. Engell and P. E. Sorensen, *Can. J. Chem.*, 1994, **72**, 2333–2338.
- 5 V. Siedlik, *Untersuchungen von Fließsystemen zur UV-spektroskopischen Bestimmung von pKs-Werten (Flowsystems in the determination of pKa-values by UV-spectroscopy)*, Bachelor Thesis, Leuphana University, Lüneburg, 2017.
- 6 S. M. Furst and J. P. Uetrecht, *Biochem. Pharmacol.*, 1993, **45**, 1267–1275.
- 7 H. Mauser, *Formale Kinetik (Experimentelle Methoden der Physik und Chemie, Band 1)*, Bertelsmann Universitätsverlag, Düsseldorf, 1974.
- 8 K. A. Connors, *Chemical Kinetics*, VCH, Weinheim, 1990.
- 9 N. Bodor, M. J. S. Dewar and A. J. Harget, *J. Am. Chem. Soc.*, 1970, **92**, 2929–2936.
- 10 C. J. T. Spitters, H. A. J. M. Toussaint and J. Goudriaan, *Agric. For. Meteo.*, 1986, **38**, 217 – 229.
- 11 M. Bindi, F. Miglietta and G. Zipoli, *Climate Res.*, 1992, **2**, 47–54.
- 12 R. G. Zepp and D. M. Cline, *Environ. Sci. Technol.*, 1977, **11**, 359–366.